Research on Engineering Structures & Materials
www.jresm.org
Research Group

Research Article

Investigation of the features of destruction of fillers of structures made of reinforced polymer composite materials

Sergey Grazion[1,a], Valery Spiryagin[*,2,b], Mikhail Erofeev[3,c], Ilnur Khuramshin[4,d], Vyacheslav Nikolenko[4,d]

[1]*JSC Corporation, Moscow Institute of Thermal Engineering, Russia*
[2]*Moscow Aviation Institute, National Research University, Russia*
[3]*Institute of Mechanical Eng. of the Russian Academy of Sciences named after A.A. Blagonravov, Russia*
[4]*26 Central Design Institute, 31 State Design Institute for Special Construction, Gagarin, Russia*

Article Info

Article history:

Received 28 June 2024
Accepted 13 Aug 2024

Keywords:

Mechanical testing;
Polymer composite materials;
Acoustic emission

Abstract

The paper presents the results of experimental studies of the destruction of fillers of polymer composite materials (PCM) with the control of acoustic emission (AE) signal parameters. As object of research were considered silica filaments K11C6-180, carbon filaments UKN-M-12K-1-7-380 and aramid technical fiber Rusar-C600 type A. Based on the experimental data obtained, acoustic emission portraits of the destruction processes of various types of PCM fillers were obtained. This allows, when loading a structure made of PCM with AE control, to fix the destruction of the filler, and, consequently, to increase the reliability and safety of operation of products made of PCM.

1. Introduction

Currently, structures made from reinforced polymer composite materials (PCM) are becoming more widely used in aviation, aerospace, and fire extinguishing systems for gas, compressed natural gas vehicles, respiratory protective equipment, and various other technological fields [1-5]. PCM comprises two main components: a filler and a binding agent. Fiberglass, carbon fibers, and organic fibers are often used as fillers in modern PCM structures. One method of nondestructive testing that allows for assessing the technical condition of a PCM structure is the acoustic emission (AE) technique [6-9].

The AE technique is based on the production of elastic waves generated during structural changes within the material, such as the formation and development of flaws in the filler or binding agent. The primary source of information is an acoustic signal, which is captured using a receiving device connected to a data acquisition and processing system. During the analysis of standard parameters (such as amplitude, duration, and rise or fall time of the acoustic emission pulse), certain criteria are calculated, based on which the level of danger posed by the acoustic signal source can be assessed.

The key advantages of this method include its high sensitivity, wide range of application possibilities, and ability to not only determine the hazard class but also locate the defect. However, a potential drawback of this approach is the registration of numerous noise signals, which can complicate the analysis process.

[*]Corresponding author: *v.v.spiryagin@yandex.ru*
[a] orcid.org/0000-0002-7040-8744; [b] orcid.org/0000-0001-6114-8138; [c] orcid.org/0000-0002-1048-3574; [d] orcid.org/0009-0007-5965-6652; [e] orcid.org/ 0009-0009-9686-018X
DOI: http://dx.doi.org/10.17515/resm2024.288cs0628rs

Currently, the AE method is used to solve a wide range of scientific and engineering problems, from corrosion control [10], fatigue and corrosion cracking of metals [11, 12] and studying the structural behavior of reinforced concrete elements [13] and critical passenger transport infrastructure facilities [14-15] to studying the patterns of formation and change of acoustic emission signals in composite materials [16-17].

The method has become widespread due to its advantages, described in detail in the works of Ivanov V.I. and Vlasov I.E. [18], Popov A.V. and co-authors [19] and a number of other researchers [20-22]. With regard to PCM, the use of traditional methods of technical diagnosis is difficult or even impossible. So, for example, the ultrasonic method has a number of disadvantages, the main of which is low sensitivity, mainly because when monitoring through an air gap, only a small part of the ultrasonic probing signal enters the product due to the large difference in acoustic resistances at the boundaries of the electroacoustic transducer — air medium and air medium — the object of control [23]. It should also be noted that the ultrasonic method is an active control method that allows you to determine only the presence of a defect, but does not provide information about its danger, including its tendency to develop and brittle destruction.

In the study [24], the authors chose radio frequency identification methods for detecting defects based on antenna deformation. However, this method does not provide information about the actual nature of the destruction of the PCM. It is rightly noted in [25] that the detection of structural damage to PCM at an early stage is impossible, since interruptions, which are damage states detected using the proposed method, occur at very high deformations - more than 20%. The main disadvantages of the proposed method include the following:

- the need to load the object, since in this state it is possible to start the process of defect development and generation of acoustic signals;
- high sensitivity to electromagnetic and acoustic interference.

Additional difficulties in the propagation of AE waves in PCM arise due to the anisotropy of the material. As a result, the signals received by the processing program can give only a limited idea of the real sources of damage. Nevertheless, these signals can still be considered sufficient for further analytical processing [26]. In [27], the authors propose a new approach to regional positioning, which allows for more accurate localization of defects. The purpose of this study is to study the characteristics of AE signals in case of failure of the PCM winding in order to develop a reliable method for monitoring the failure processes of both the entire PCM structure and individual components, in particular, the filler.

Table 1. Physico-mechanical properties of silica threads К11С6-180

Material	Linear density (tex)	Twist amount (tw/m)	Breaking load (N(kgf), not less)
К11С6-180	1014.22	1099.71	23.1

The aim of this study is to investigate the characteristics of AE signals during the failure of PCM winding, in order to develop a reliable method for monitoring the failure processes of both the overall PCM structure and individual components, specifically the filler. The silica К11С6-180 fibers, carbon UKN-M-12K-1-7-380fibers, and technical fiber Rusar-C600 of the A brand are the objects of this investigation. In the following, we will refer to these materials using their Russian labels. With respect to their physical and mechanical properties, these materials meet the specifications outlined in Tables 1-3.

Table 2. Physico-mechanical properties of carbon threads UKN-M-12K-1-7-380Э,Д

Material	Thread density, (g/cm3)	Specific breaking load of thread when breaking loops, (cN/tex, not less)	Elastic modulus, (GPa)	Breaking stress of an elementary thread (filaments) under tension, (GPa, not less)
UKN-M-12K-1-7-380	1.75±0.04	10	225±20	3.5

Table 3. Physico-mechanical properties of aramid technical fiber Rusar-C600

Material	Linear density (tex)	Number of threads in the fiber, pcs	Breaking load (N(kgf), not less)	Dynamic modulus of elasticity of complex thread, GPa, (kgf/mm2), not less	Twist of filament thread, tw/m
Rusar-C600A	1.75±0.04	10	225±20	3.5	

2. Materials and Methods

To investigate the process of filament destruction while monitoring AE signal parameters, a testing setup was developed, the appearance of which is depicted in Fig. 1. The main components of the experimental set-up are: 1 a loading device; 2 an acoustic emission system, UNISCOPE; 3 the object of study; 4 acoustic emission converters (AEC) of the GT200 and GT205 types; 5 waveguide grips. The main challenge in setting up the experiment was ensuring the acoustic contact between the object under study, in this case the filaments, and the AEC. To achieve this, we designed and tested the waveguide grips shown in Fig. 1b. The waveguide grip is composed of two plates and four screws. The working plate is made of steel. The main parameters of the waveguide were selected based on the following criteria: 1) the frequency range of operation is 30-300 kHz; 2) the controllers used are DR15I, DR6I from the MALACHITE system or GT200 and GT205 from UNISCOPE; 3) an average wave speed of approximately 3000 m/s as recorded by AEC devices. Based on these criteria, the wavelength lies in the range of 1.5-6 cm.

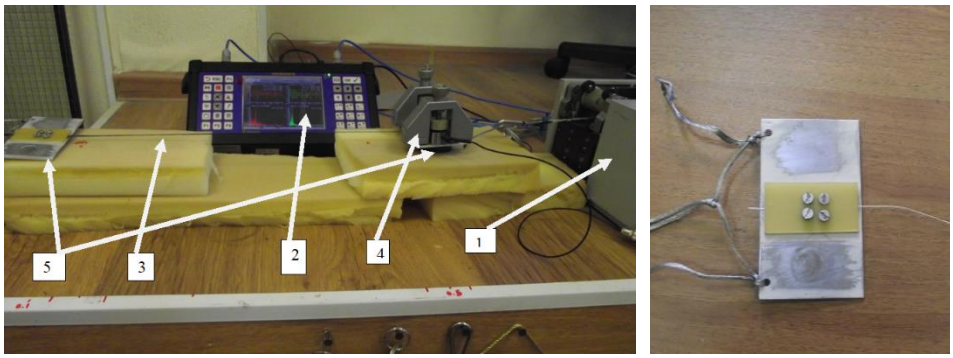

Fig. 1. Experimental setup: left general view; right waveguide grip

Based on this information, the dimensions of the work plate are 115 x 65 x 3 mm. These dimensions allow for the installation of AEC DR15I, DR6I, or GT200, GT205 using magnetic clamps, as shown in Figure 2. The thickness of the waveguide should be commensurate with the wavelength, in order to ensure optimal performance. The characteristics of the AEC used in this study are presented in Table 4.

Fig. 2. AEC is used in conjunction with a waveguide grip

The second plate is manufactured from a material with a high level of attenuation and is designed to apply pressure to the thread. The high attenuation of acoustic signals within the pressure plate results in a significant reduction of the reverberant component when the signal travels through the pressure plate. For the study, 70 mm-long threads were utilized. The ends of the threads were bonded at each end, approximately 10 cm apart, using butyral phenolic glue (BF adhesive), in accordance with Russian standards for determining breaking strength and elongation upon rupture of textile fiber materials (GOST 6943-79).

Table 4. Characteristics of AEC

#	Characteristics	Type of acoustic emission converter			
		DR6I AT	DR15I AT	GT200	GT205
1	Nominal resonant. frequency, kHz	60	150	165	50
2	Operating frequency range, kHz	30–120	75-300	100-200	40-100
3	Gain, dB	34	34	20	20
4	Supply voltage, V	15	15	6	6
5	Dimensions without cable (diameter/height, mm	28 □ 38	28x32	16x15	
6	Weight, g	100	90	14	22x25,5
7	Tread material	Ceramics			
8	Execution	hermetically			

The ends of the glued threads were positioned between the plates, with the protruding end being approximately 2-3 centimeters in length, and secured with screws. An AEC was mounted on the receiving waveguide using an acoustically transparent lubricant. One end of the waveguide was fixed to a stationary support, while the other end was connected to a loading device. The thread was pulled with a force of approximately 2-2.5 kilograms. AE signals were generated for testing. The Su-Nielsen simulator was utilized as a substitute. The signals were produced on a waveguide equipped with an AEC, as well as on a filament located at distances of 10, 20, 30, 40, and 50 centimeters from the receiving waveguide. Prior to simulating the signal on the filament, a rigid support was positioned beneath it near the point of simulation in order to eliminate any vibrations in the filament as a string. Consequently, an attenuation curve for acoustic signals was derived, as shown in Figure 3. The "0" distance corresponds to the amplitude of signals when simulated on the receiving waveguide with an AEC.

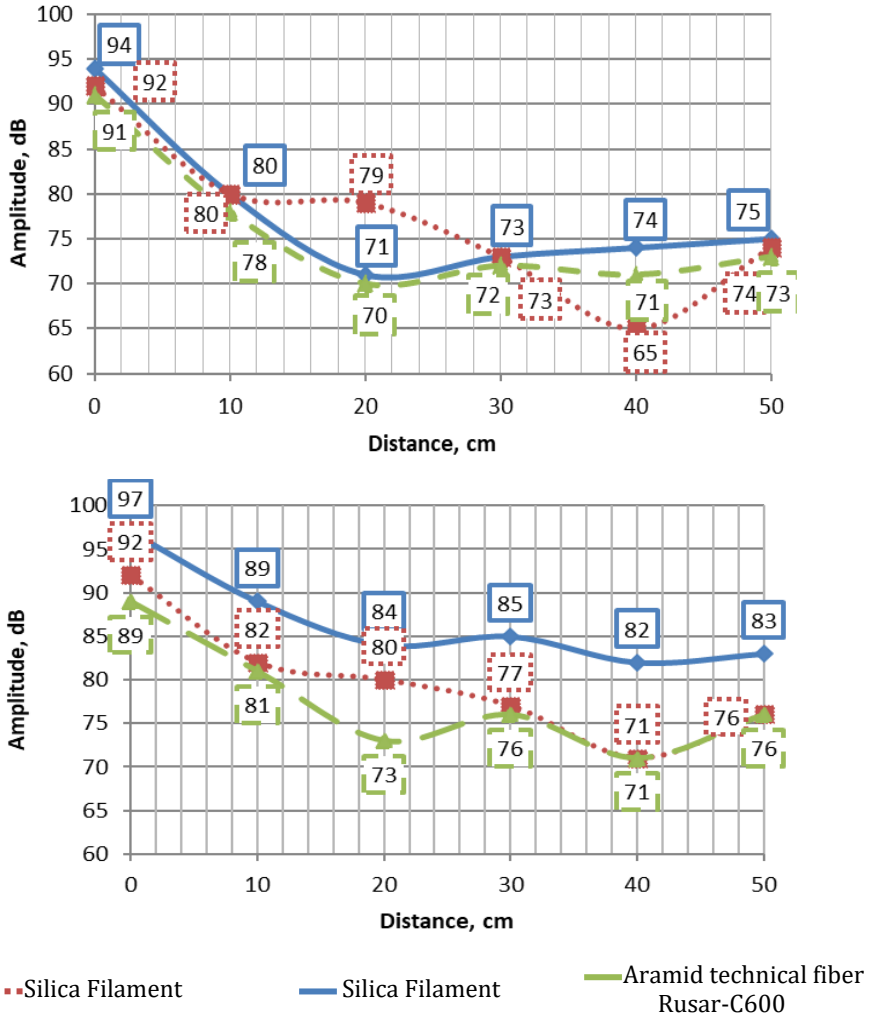

Fig. 3. Decay curves when recording signals: top – AEC GT200; below – AEC GT205

It can be observed from the attenuation curves that:

- the attenuation of signals during the transition from filaments to waveguide is approximately 12-14 dB for AEC GT200 and 8-10 dB for GT 205;
- signal attenuation during propagation in filaments:
- in silica filaments, the order of attenuation is 10 dB/m for GT200 and 12 dB/m for GT205; In carbon filaments, it is approximately 12 dB/m for GT200 and 10 dB/m for GT205;
- the technical fiber attenuation of the Rusar-C600A is approximately 8 dB/m for GT200 and 10 dB/m for GT205.

Amplitude-frequency characteristics (frequency response) of AEC GT205 and GT200, when simulating signals on waveguide capture and filament, at a distance of 10 and 40 cm from waveguide capture, are shown in Figures 4-6.

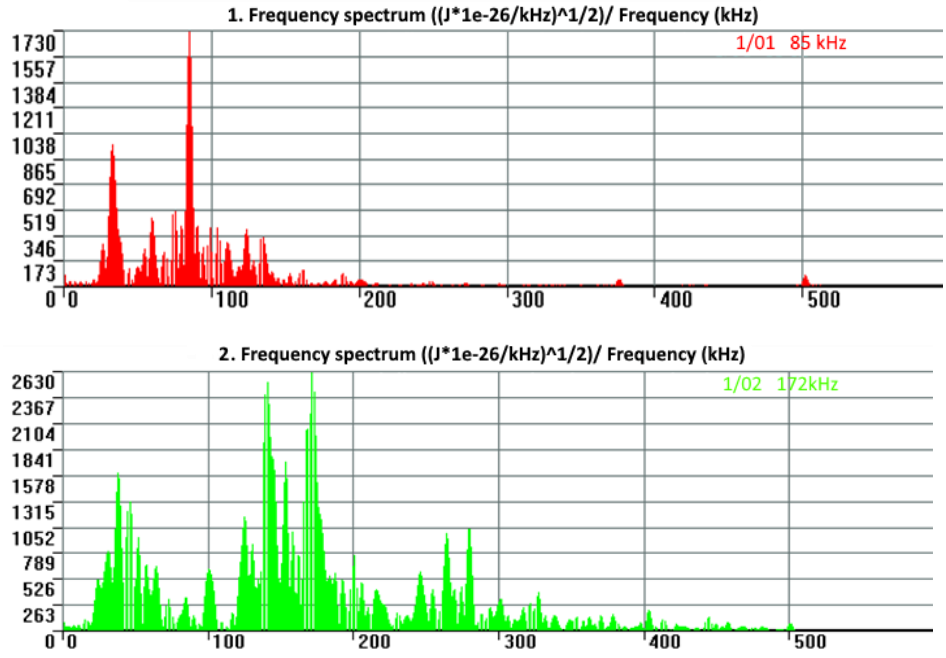

Fig.4. Amplitude-frequency characteristics when recording GT205 (top) and GT200 (bottom) signals when simulating signals on a waveguide grip

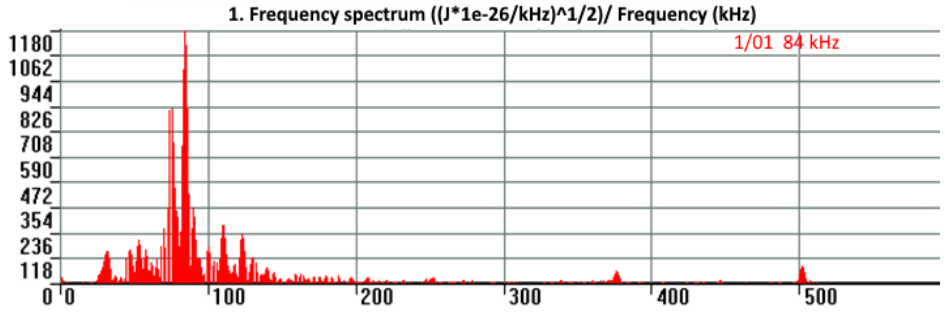

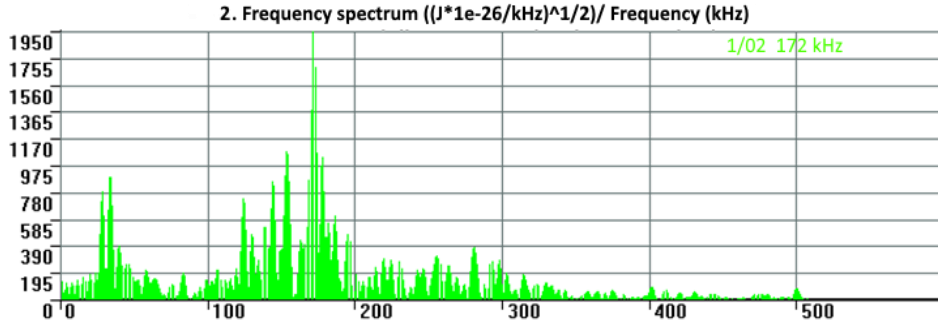

Fig. 5. Amplitude-frequency characteristics when recording GT205 (top) and GT200 (bottom) signals when simulating signals on a filament at a distance of 10 cm from the waveguide grip

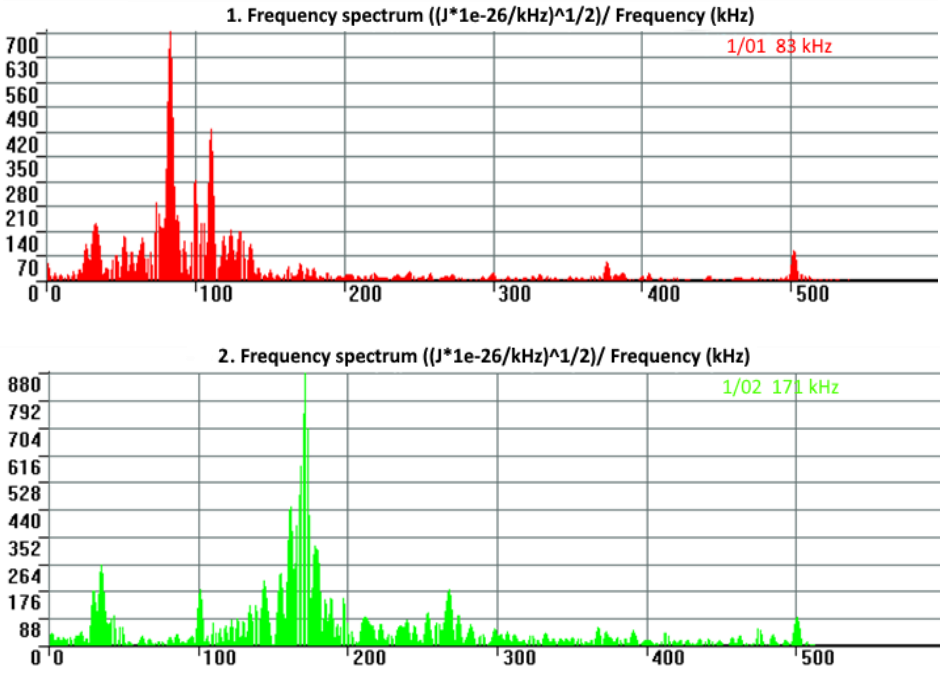

Fig. 6. Amplitude-frequency characteristics when recording GT205 (top) and GT200 (bottom) signals when simulating signals on a filament at a distance of 40 cm from the waveguide grip

A comparison of the frequency response when simulating signals on the capture waveguide and on the filament shows the absence of distortion of the recorded signals during the transition from the filament to the waveguide for AEC GT205 and GT200. For example, Fig. 4-6 shows the frequency response for Rusar-C600A technical fiber. The frequency response for silica and carbon filaments is similar. The same installation was used to determine the propagation velocity of ultrasonic vibrations in the threads and technical fiber. At the same time, the distance between the AEC is 1000 mm and three grippers were used. Two grippers were used, among other things, as waveguides on which the AEC was installed, the third gripper (pads. 1 in Fig. 7) was used to tighten the section

of threads on which the AE signals were simulated (Su-Nilsson source). It has been established that the acoustic wave propagation velocity is on the order of 1422 m/s for silica filament, 2099 m/s for carbon filament and 1805 m/s for a technical fiber.

Using the above setup, the parameters of AE signals arising from the destruction of filaments were studied. Threads and a 500 mm long tourniquet were used for the study. The threads and the technical fiber were loaded to destruction with simultaneous registration of AE signals using AES GT205 and GT200. Changes in the average amplitude and AE activity were selected as acoustic emission parameters, which serve as an acoustic emission portrait of a specific material. The amplitude parameter of acoustic signals directly depends on the properties of the material and allows you to reliably determine its type against the background of external noise and/or concomitant destruction of materials (for example, simultaneous destruction of the liner material and the power shell of a metal-composite high-pressure cylinder) [9]. Apply AE activity to PCM, that is, the number of registered pulses of acoustic emission per unit of time, gives an idea of the structure of the material. Thus, when fibrous materials are destroyed, the activity will be higher due to the generation of acoustic signals from the destruction of single fibers.

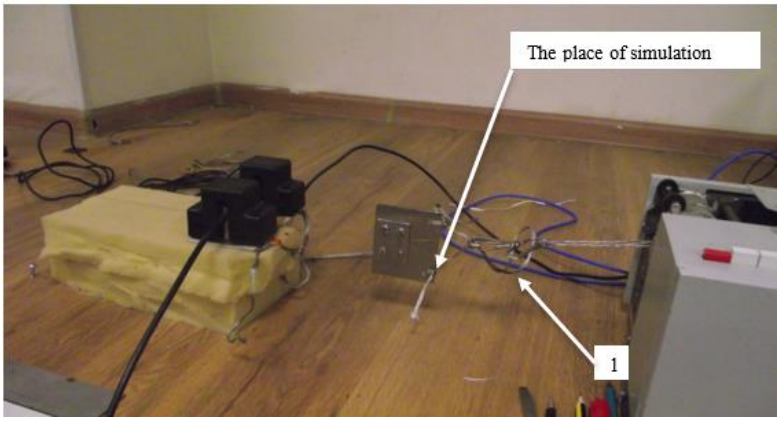

Fig. 7. Experimental setup for determining the speed of propagation of ultrasonic vibrations

3. Results and Discussion

Analyzing the dynamics of changes in the parameters of AE signals during destruction, it can be noted that such parameters as the average amplitude and activity allow us to conclude about the type of collapsing filaments. Figure 8 shows generalized graphs of changes in the average amplitude during the destruction of the filaments and technical fiber, and Figure 9 shows graphs of changes in AE activity. A sign of the failure of the Rusar -C600 technical fiber, in the context of the failure of silica and carbon fibers, is the detection of pulses with amplitudes exceeding 70 decibels. A sign of failure of carbon fibers, in the presence of failed silica fibers and the technical fiber, is the recording of acoustic emission (AE) activity exceeding 50 events per second.

The nature of the variation in the temporal characteristics of AE pulses (mean duration and mean rise time) is consistent across all samples. Graphs depicting the relationship between the mean rise time and the duration of the pulses are presented in Figure 10.

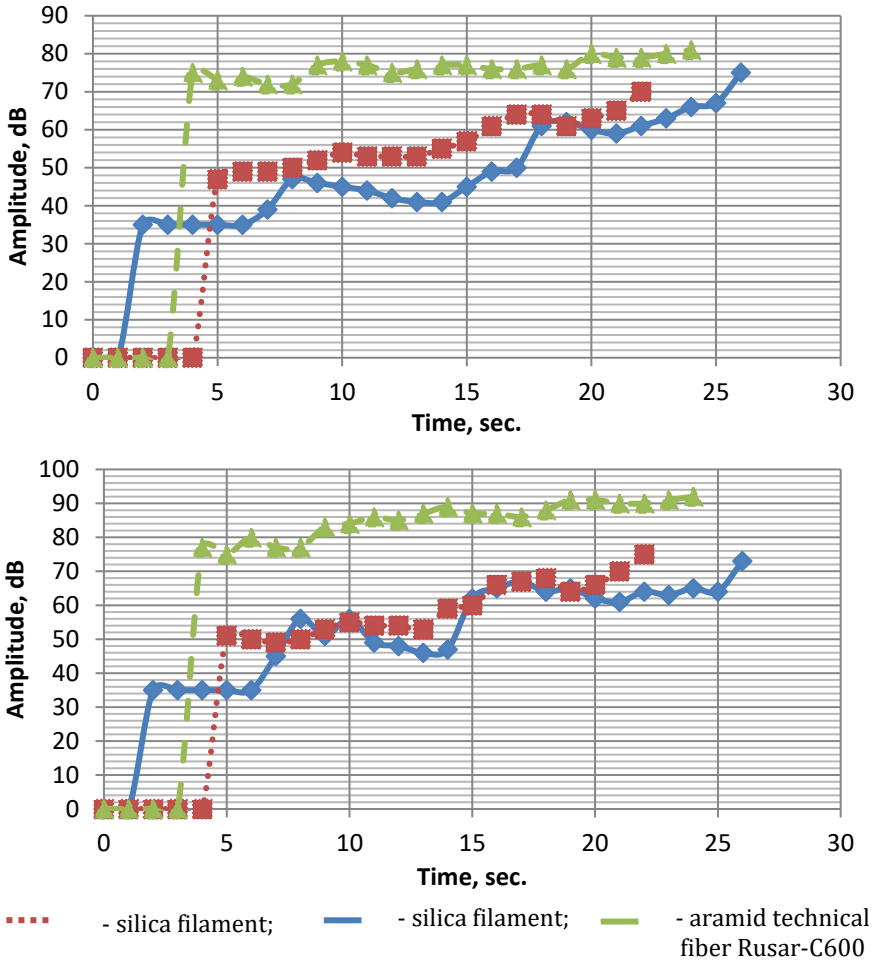

Fig. 8. Graphs of changes in the average amplitude during the destruction of filaments and technical fibers: top - AEC GT200; below is the AEC GT205

Silica filaments are characterized by a high ratio at the initial and final moment of destruction. Carbon filaments are characterized by a small ratio range, lying in the range of 0.28-0.38. Aramid technical fiber is characterized by a spread from 0.1 to 0.3. I.e., the harness is characterized by a short pulse rise time. The destruction occurred by sequential destruction of individual groups of elementary strands during the order of 23-26 seconds. The appearance of the destroyed fibers and the aramid technical fiber are shown in Fig. 10.

The destruction of the threads was fragile, which is confirmed by the enlarged images in Figure 10. The analysis of the frequency response at the rupture of filaments for EACH GT205 and GT200 (Fig. 12-14) showed that the highest energy is recorded when the technical fiber is destroyed, and the lowest when the silica filament is destroyed. The energy released in the low-frequency spectrum is concentrated in the frequency range of 50-120 kHz, in the high-frequency spectrum it is concentrated in the range of 140-300 kHz, while in the range of 50-120 kHz the amount of energy released is almost 3-5 times higher.

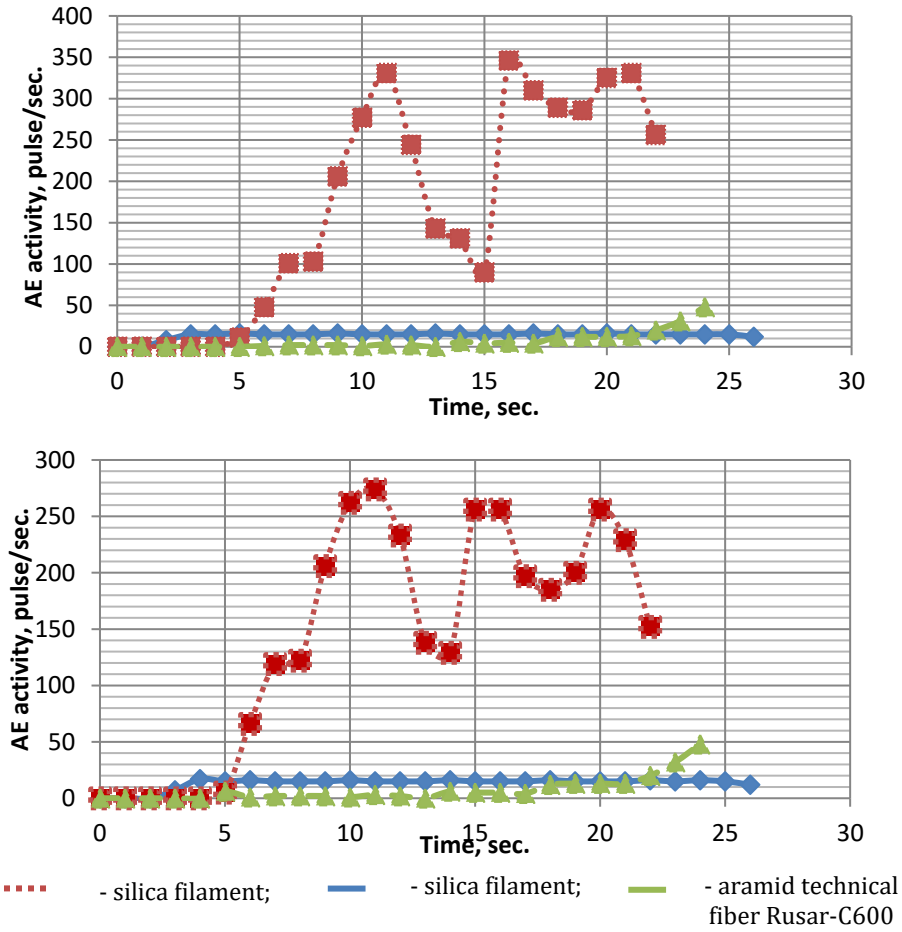

Fig. 9. Graphs of changes in AE activity during the destruction of filaments and technical fibers: top – AEC GT200; below is the AEC GT205.

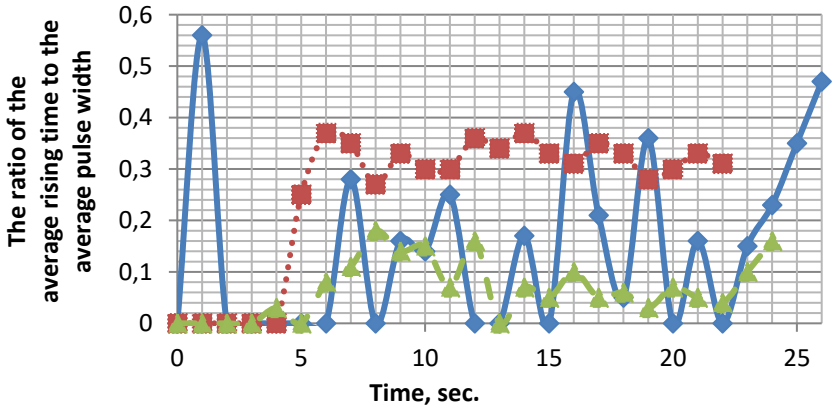

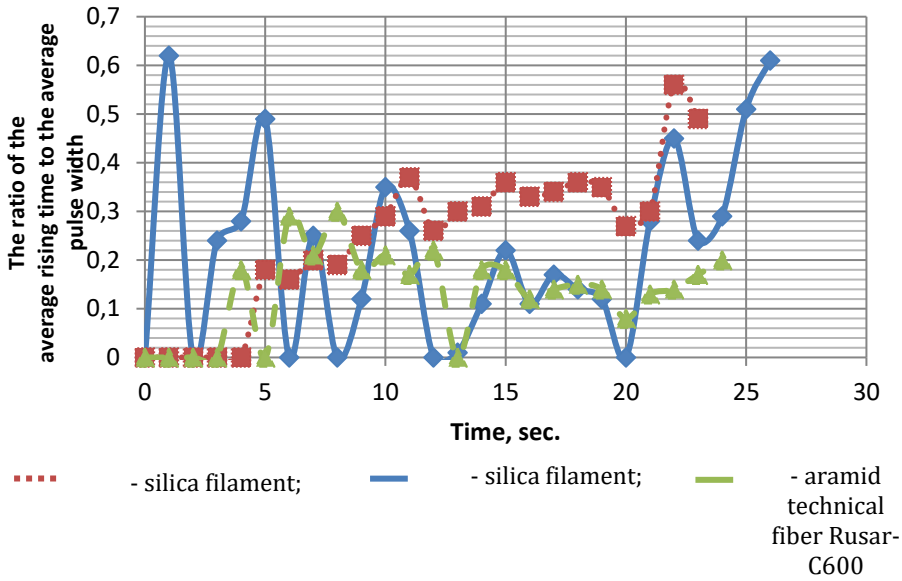

Fig. 10. Ratios of the average rise time of pulses to their average duration: top – AEC GT200; below is the AEC GT205

Fig. 11. Appearance of destroyed filaments and technical fiber, 1) silica filament; zoom in x182 on the right; 2) carbon filament; zoom in x102 on the right; 3) aramid technical fiber Rusar-C600; zoom in x139 on the right

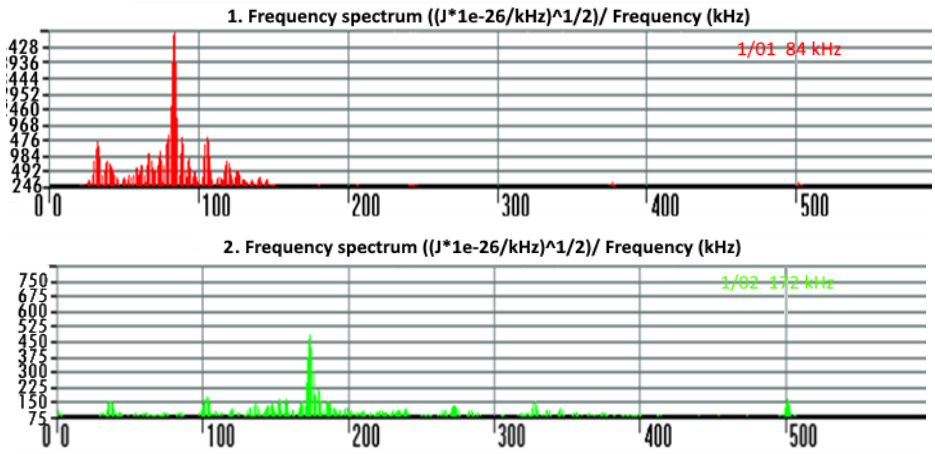

Fig. 12. Amplitude-frequency characteristics when silica filament breaks: top - GT205; below GT200

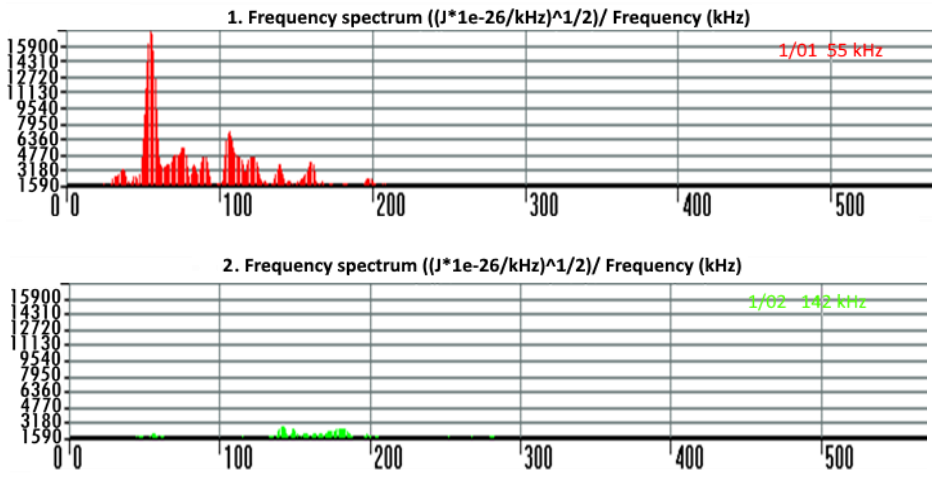

Fig. 13. Amplitude-frequency characteristics when carbon filament breaks: top - GT205; below GT200

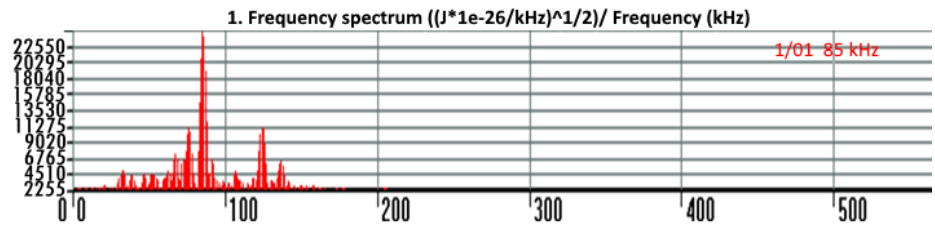

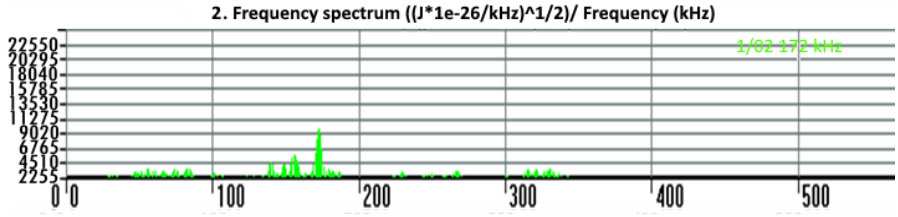

Fig. 14. Amplitude-frequency characteristics when aramid technical fiber Rusar-C600 breaks: top - GT205; below GT200

5. Conclusions

The study confirmed the possibility of detecting cases of destruction of the filler when loading of the of structures made of reinforced polymer composite materials and determining the type of destroyed filler of reinforced structures made of PCM. The obtained data on the features of the destruction of fillers allowed us to obtain an acoustic emission portrait of the destruction of reinforced PCM materials, which allows us to conclude about the type of collapsing filaments according to the following distinctive features:

- A sign of the destruction of technical fiber Rusar – C600A against the background of the destruction of silica and carbon filaments is the registration of pulses with an amplitude of more than 70 dB.
- A sign of the destruction of carbon filaments against the background of the destruction of silica and technical fiber filaments is the registration of AE activity above 50 imp/sec.
- An additional feature in case of destruction is the energy parameter: the highest energy is recorded when the technical fiber is destroyed, and the lowest when the silica filament is destroyed.

It was also found that the most informative frequency range for recording AE signals in PCM is the 40-120 kHz range. In order to register AE signals arising from the destruction of carbon or silica filaments, it is advisable to use PAE type GT205 or DR6I.Thus, the use of the acoustic emission control method makes it possible not only to assess the technical condition of PCM products, but also to predict their performance due to the possibility of early detection of hidden developing defects, such as the destruction of single fibers of silica or carbon filaments. In the complex with the research of the parameters of acoustic emission signals during the destruction of the liner material and the power shell of a metal-composite high-pressure cylinder [9], acoustic emission parameters of AE signals arising from the destruction of filaments of PCM fillers, binder, micro composite and liner metal were obtained. The obtained acoustic emission portrait is an integral part of the development of a program for technical diagnostics of products made of PCM and will be used in the further development of criteria for evaluating AE sources in accordance with their degree of danger.

References

[1] Markin V, Myagkova N. High-pressure cylinders of gas-fuel system made of composite materials. IOP Conf Ser Mater Sci Eng. 2021;1100:012011. https://doi.org/10.1088/1757-899X/1100/1/012011

[2] Chauhan G, Awasthi A. Design and analysis of high-pressure composite vessels. Int J Latest Eng Manag Res. 2018;03(06):96-102.

[3] Stepanova L, Ramazanov I, Chernova V. Acoustic and emission analysis of the defect nucleation process in carbon fiber reinforced plastic samples. Transp Res Procedia. 2021;54:320-327. https://doi.org/10.1016/j.trpro.2021.02.078
[4] Берлин АА, редактор. Полимерные композиционные материалы: структура, ствойства, технология: учеб пособие. 3-е испр. изд. СПб.: ЦОП «Профессия»; 2011. 560 с.
[5] Lebedev IK, Lebedev KN, Moroz NG. Experimental studies of life characteristics of metal-composite cylinders. Civil Aviat High Technol. 2015;(212):137-142. (In Russ.).
[6] Bo K, Liu S, Cheng L, Yuan Y, Luo H. Experiment research on acoustic emission of impact-damaged fully-wrapped composite gas cylinder with non-metallic liner. In: Proceedings of the 14th International Conference on Non-destructive Testing in Aerospace; 2021; Berlin, Germany. https://doi.org/10.1007/978-981-15-9837-1_33
[7] Jiang P, Liu X, Li W, et al. Damage characterization of carbon fiber composite pressure vessels based on modal acoustic emission. Materials. 2022;15:4783. https://doi.org/10.3390/ma15144783
[8] Ono K, Gallego A. Research and applications of ae on advanced composites. J Acoust Emiss. 2012;30:180-220.
[9] Erofeev M, et al. The effects of ultrasonic treatment on the structure and properties of alloys. J Phys Conf Ser. 2021;2131:022062. https://doi.org/10.1088/1742-6596/2131/2/022062
[10] Hua W, Chen Y, Zhao X, et al. Research on corrosion detection method of oil tank bottom based on acoustic emission technology. Preprints. 2024; 24: 3053. https://doi.org/10.20944/preprints202404.0165.v1
[11] Bhuiyan MY, Lin B, Giurgiutiu V. Acoustic emission sensor effect and waveform evolution during fatigue crack growth in thin metallic plate. J Intell Mater Syst Struct. 2018;29(7):1275-1284. https://doi.org/10.1177/1045389X17730930
[12] Bi HS, Li HY, Zhang W, et al. Evaluation of the acoustic emission monitoring method for stress corrosion cracking on aboveground storage tank floor steel. Int J Press Vessels Pip. 2020;179:7. https://doi.org/10.1016/j.ijpvp.2019.104035
[13] Manthei G, Koob M, Walther M, Minnert J. Analysis of the structural behavior of reinforced concrete components with acoustic emission analysis. e-J Nondestruct Test. 2024;29. https://doi.org/10.58286/29893
[14] Zhang J, Shen G, Chen D, et al. Application of acoustic emission technology for bearing condition monitoring on passenger ropeway. e-J Nondestruct Test. 2024;29.
[15] Liu R, Liang YJ, Liu S, et al. Applicability of a new composite amusement ride safety device based on acoustic emission monitoring technology. Mater Res Express. 2024;11. https://doi.org/10.1088/2053-1591/ad43c0
[16] Filonenko S, Stakhova A, Bekö A, Grmanova A. Acoustic emission during non-uniform progression of processes in composite failure according to the Von Mises Criterion. J Compos Sci. 2024;8:235. https://doi.org/10.3390/jcs8070235
[17] Wei D, Yang Y, Si J, Wen X. Study on acoustic emission detection technology of fiber reinforced plastic pressure vessel. In: ASME Pressure Vessels and Piping Conference. 2020. https://doi.org/10.1115/PVP2020-21088
[18] Ivanov VI, Vlasov IE. Acoustic emission method. In: Klyuev VV, editor. Non-destructive testing: Handbook. Vol. 7. Book 1. Moscow: Mechanical Engineering; 2005; page 340.
[19] Popov AV, Voloshina VYu, Zhuravsky KA, Labina MA. Acoustic emission method of diagnostics of structures made of composite materials based on invariants. Adv Eng Res. 2022;22(4):331-337. https://doi.org/10.23947/2687-1653-2022-22-4-331-337
[20] Lyu NT, Nguyen KD, Demchenko SK, Chernoverskaya VV. Application of the acoustic emission method in problems of control and monitoring of the technical condition of diagnosed objects. In: Proceedings of the International Symposium "Reliability and Quality"; 2021; 2:77-82.

[21] Zaki A, Chai HK, Behnia A, et al. Monitoring fracture of steel corroded reinforced concrete members under flexure by acoustic emission technique. Constr Build Mater. 2016. https://doi.org/10.1016/j.conbuildmat.2016.11.079
[22] Ono K. Application of acoustic emission for structure diagnosis. Konferencja Naukowa. 2010; pp.317-341.
[23] Kachanov VK, Sokolov IV, Karavaev MA, Kontsov RV. Selecting optimum parameters of ultrasonic noncontact shadow method for testing products made of polymer composite materials. Russ J Nondestruct Test. 2020;56(10):831-842. https://doi.org/10.1134/S1061830920100046
[24] Korzec I, Samborski S, Łusiak T. A study on mechanical strength and failure of fabric reinforced polymer composites. Adv Sci Technol Res. 2022;16:120-130. https://doi.org/10.12913/22998624/146686
[25] Pecho P, Hrúz M, Novák A, Trško L. Internal damage detection of composite structures using passive RFID tag antenna deformation method: basic research. Sensors. 2021;21(24):8236. https://doi.org/10.3390/s21248236
[26] Fowler TJ, Gray E. Development of an acoustic emission test for FRP equipment. In: Preprint 3583, American Society of Civil Engineers; 1979.
[27] Wei D, Yang Y, Si J, Wen X. Study on acoustic emission detection technology of fiber reinforced plastic pressure vessel. 2020. https://doi.org/10.1115/PVP2020-21088